Balhassn S. M. Ali*

The Pin-Loaded Small One-Bar Specimen in Use to Determine Uniaxial and Multiaxial Creep Data

DOI 10.1515/htmp-2015-0029
Received February 1, 2015; accepted September 18, 2015

Abstract: Two novel small specimen creep testing techniques are presented in this paper. The pin-loaded small one-bar specimen (OBS) and the small notched specimen with four loading pins (SNS4) are designed to determine the remaining lifetime for the high-temperature components. The small OBS is suitable for use in obtaining both uniaxial creep strain and creep rupture life data and the SNS4 is designed to obtain the multiaxial behaviour using small material samples. The specimens can be made from small material samples removed from the component surface or from the heat-affected zone. The specimens can be loaded through pin connections for testing. A conversion relationship and conversion factor have been obtained and used to convert the OBS creep data to the corresponding uniaxial data. For validation two materials have been used, P92 and P91 steels at 650°C. The advantages of these testing techniques are highlighted; the recommendations for future research are also given.

Keywords: small one-bar specimen, small notched specimen, conversion factors, conversion relationship, creep assessment

Introduction

Many of the engineering components in chemical plants, power generation plants, aero-engines and oil refineries operate at temperatures and/or stresses which are high enough to cause creep to occur [1–3]. Creep failure of these components normally leads to significant damage financially, environmentally as well as the loss of human lives in most cases. In order to improve safety, efficiencies and lower emissions and fuel consumption, new materials are being introduced to the industries mentioned above and these materials are being subjected to increasingly severe loading conditions (see [4–6]). In order to ensure the safe operation of components, improved understanding of the creep behaviour of the materials being used to manufacture them and improved inspection techniques are required [1, 7, 8]. One effect of the desire to improve understanding of material behaviours and to obtain better inspection techniques is the need, in some cases, to uses small material samples [9–10]. This comes about because small scoop samples (see Figures 1 and 2) with depth of 3 mm and radius of 15 mm can be removed from some components, for example, steam pipes and pipe bends in the power plants, without adversely affecting their safe operation. Also, for some material zones, for example, the heat-affected zones (HAZ) of welds, only small amounts of material are available for testing.

A conventional cylindrical uniaxial creep test specimen (see Figure 3) with total length of about 130 mm and diameter of 16 mm, or the Bridgeman notched specimen (see Figure 8) cannot be manufactured out of a typical scoop sample or from the HAZ region of weld because the scoop samples and the HAZ region are far too small to allow these specimens to be extracted from them. Therefore, it has become necessary to develop small specimen creep testing techniques, whereby reliable creep data can be obtained using small material samples [11–13]. The limitations associated with the previous small specimens creep testing techniques made them unable to replace the uniaxial and the Bridgeman notched specimens when there is not enough material for creep assessment. However, pin-loaded small one-bar specimen (OBS) and the small notched specimen with four loading pins (SNS4) presented in this paper are designed to overcome the limitations associated with the previous small specimen creep testing techniques.

Specimen geometries and dimensions

The primary objective of this research is to develop the non-destructive small specimen creep testing technique which can be used to assess creep strength and to determine the remaining lifetimes for the high-temperature

***Corresponding author: Balhassn S. M. Ali,** Department of Mechanical and Industrial Engineering, Bursa Orhangazi University, Bursa, Turkey, E-mail: balhassn.ali@bou.edu.tr

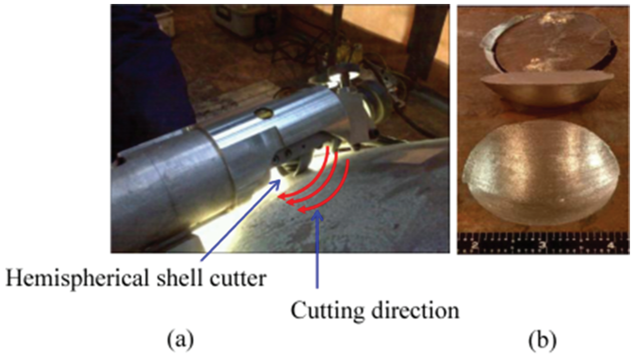

Figure 1: Photographs of scoop sampling in process on stem pipe (a), and image of a typical scoop sample (b).

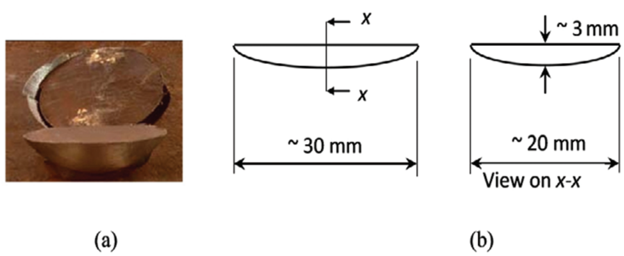

Figure 2: Dimensions of a typical scoop sample.

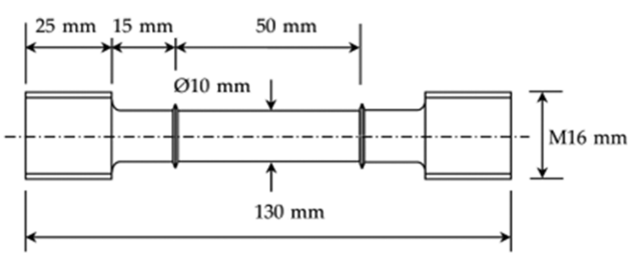

Figure 3: Conventional uniaxial creep test specimen.

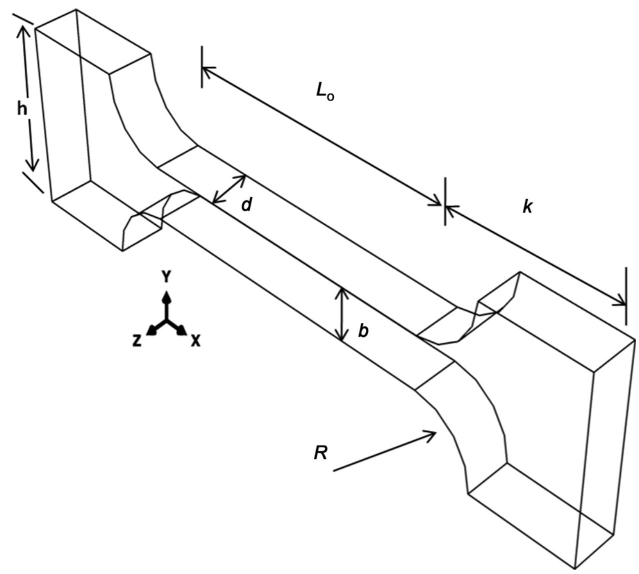

Figure 4: The pin-loaded small one-bar specimen (OBS) shape and dimensions, where L_o is the distance between the centres of the loading and constraining pins (~(5–13) mm), *K* is the supporting material behind the loading pins (~(2–4) mm), *R* is the loading pin radius (~(1–2) mm), *b* is the bar thickness (~(1–2) mm), *d* is the specimen depth (~(1–2) mm) and *h* is the specimen height (~(3.5–7) mm).

components using small material samples. The proposed pin-loaded small OBS and the SNS4 are designed to determine the creep strength and the remaining lifetime for the high-temperature engineering components, using small material samples. The OBS type (see Figures 4 and 5) and SNS4 (see Figures 6 and 7) have simple geometries, therefore they can be easily manufactured using, for example, electric discharge machining (EDM). The OBS specimen dimensions are defined by L_o, *b*, *d*, *h*, *R* and *k*, where L_o is "bar" length, i.e. the distance between the centres of the loading pins in the loading direction, *b* is the bar width, *d* is the specimen thickness, *h* is the specimen height, *R* is the radius of the loading pins and *k* is the length of the loading pin supporting end, as shown in Figure 4. The small OBS is designed to replace the uniaxial creep test specimen (see Figure 3) when there is not enough material available for testing. The OBS is capable

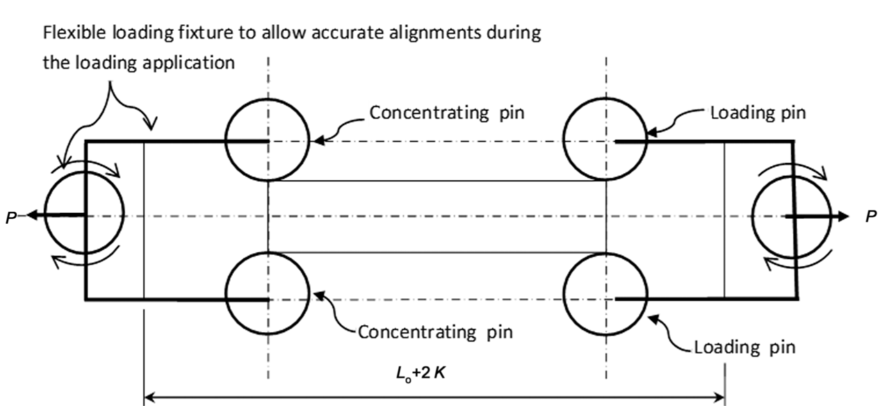

Figure 5: The pin-loaded small one-bar specimen (OBS) with the loading and constraining pins in position.

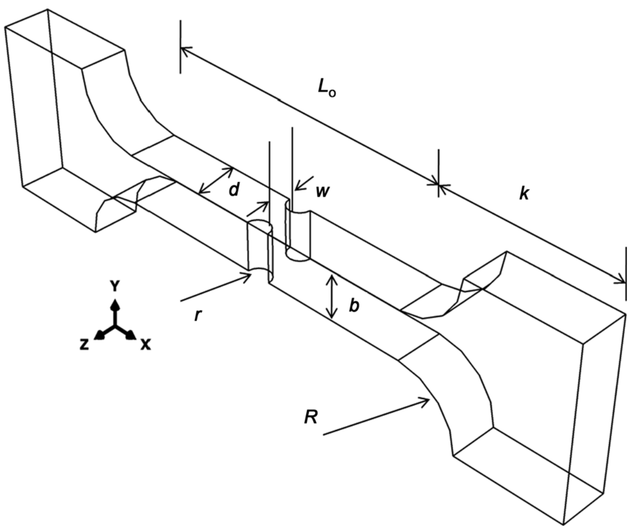

Figure 6: The small notched specimen with four loading pins (SNS4) shape and dimensions, where L_o is the distance between the centres of the loading and constraining pins (~(6–13) mm), K is the supporting material behind the loading pins (~(2–4) mm), R is the loading pin radius (~(1–2) mm), r is the notch radius (~(0.5–1) mm), b is the bar thickness (~(1–2) mm) and d is the specimen depth (~(1–2) mm).

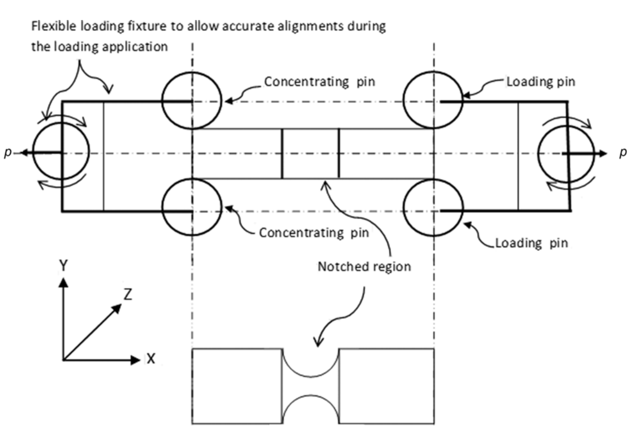

Figure 7: The small notched specimen with four loading pins (SNS4) with the loading and constraining pins in position.

of obtaining uniaxial creep strain and creep rupture data using small material samples. The OBS is unlike other small specimen creep testing techniques, it is capable of obtaining the full creep strain-time curves, i.e. primary, secondary and tertiary regions, similar to the strain-time curves obtained from the uniaxial creep test specimens.

Most of the high-temperature components in the power plants operate under multiaxial stress state condition and not just under uniaxial condition, therefore the multiaxial stress state for the material needs to be defined in order to obtain accurate creep assessment for

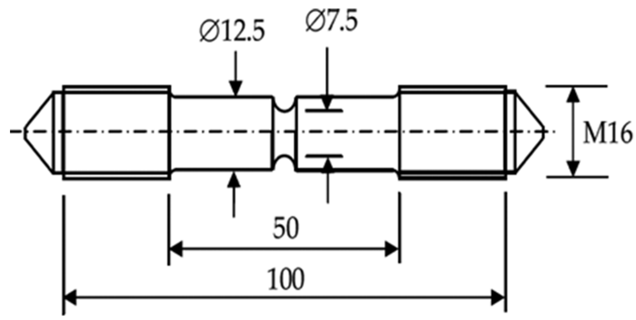

Figure 8: Conventional Bridgeman notched bar specimen.

the components. Traditionally the Bridgeman notched specimen is used (see Figure 8) to determine the multiaxial stress state parameter; however, in many cases the material available for creep assessment is not enough to manufacture this specimen type; the proposed SNS4 specimen can be used instead in such cases. The SNS4 dimensions are defined by L_o, r, b, d, h, R and k, where L_o is “bar” length, i.e. the distance between the centres of the loading pins in the loading direction, r is the small notch radius, b is the bar width, d is the specimen thickness, h is the specimen height, R is the radius of the loading pins and k is the length of the loading pin supporting end, as shown in Figures 6 and 7. Most of the components operating under creep condition are subject to multiples stresses, not only stresses in the directions of X–Y coordinate, but also subject to stresses in many other directions, normally referred to as the multiaxial stress. The SNS4 has been designed to obtain only the multiaxial stress state parameter for the high-temperature material. The multiaxial stress state parameter for the material at a particular temperature can be obtained by comparing the SNS4 experimental failure times with the corresponding finite element (FE) analyses failure time; this procedure has been explained and published in Ref. [14].

Data conversion method

Stress and strain for uniaxial specimens

To determine the stress level for the conventional uniaxial creep test specimen, the applied load is divided by the cross-section area of the specimen, i.e.

$$\sigma = \frac{P}{A} \quad (1)$$

where σ is the nominal stress, P is the applied load and A is the cross-section area, i.e. $A = \pi r^2$, for the case of cylindrical uniaxial specimen. Similarly the creep strain ε^c for the conventional cylindrical uniaxial specimen can be calculated by dividing the specimen extension by the original length, i.e.

$$\varepsilon^c = \frac{L2 - L1}{L1} \quad (2)$$

and $L_2 - L_1 = \Delta^c$, in the case of tensile loading creep test, where L_1 is the original gauge length (GL), L_2 is the new length after the extension, Δ^c is creep displacement and ε^c is creep strain. However, in this case where non-conventional creep specimen (e.g. the small OBS) is used, these two relationships, i.e. eqs (1) and (2), cannot be used, because of two reasons:

(i) The specimen is loaded using loading pins, therefore the applied load will be transferred to the specimen bar (the uniform part L_o) through the loading pin supporting material, i.e. dividing the applied load P by the specimen bar cross-section area (A) will not be equal to the nominal stress (σ_{nom}) in the specimen bar.

(ii) The deformation in the OBS supporting material behind the loading pins makes the OBS strain higher than the conventional creep specimen strain for the same GL (L_o). The creep deformation in the OBS case is a combination of two deformations, i.e. $\Delta^c = \Delta^c_{\mathrm{Lo}} + \Delta^c_k$, where Δ^c_{Lo} is the dominant creep deformation in the specimen bar and Δ^c_k is the additional deformation in the supporting material behind the loading pins. These two issues have been solved using the reference stress method (RSM) and the FE analyses method.

Creep deformation and RSM

For some components and loading modes, it is possible to obtain analytical expressions for steady-state creep deformation rates, $\dot{\Delta}_{\mathrm{ss}}$ [14–17]. For a material obeying Norton's power law, i.e. $\dot{\varepsilon}^c = A\sigma^n$, these show that the general form is

$$\dot{\Delta}^c_{\mathrm{ss}} = f_1(n) f_2(\mathrm{dimension}) A(\sigma_{\mathrm{nom}})^n \quad (3)$$

where f_1 (n) is a function of the stress index, n, f_2 (dimensions) is a function of the component dimensions and σ_{nom} is a conveniently determined nominal stress for the component and loading.

By introducing an appropriate scaling factor, α, for the nominal stress, eq. (3) can be rewritten as

$$\dot{\Delta}^c_{\mathrm{ss}} = \frac{f_1(n)}{\alpha^n} f_2(\mathrm{dimension}) A(\alpha\sigma_{\mathrm{nom}})^n \quad (4)$$

Choosing α $(=\eta)$ so that $f_1(n)/(\eta)^n$ is independent (or approximately independent) of n, then eq. (4) can be further simplified, i.e.

$$\dot{\Delta}^c_{\mathrm{ss}} \approx D\dot{\varepsilon}^c(\sigma_{\mathrm{ref}}) \quad (5)$$

where D is the so-called reference multiplier [$D = (f_1(n)/\eta^n)$ f_2 (dimensions)] and $\dot{\varepsilon}^c(\sigma_R)$ is the minimum creep strain rate obtained from a uniaxial creep test at the so-called reference stress, i.e.

$$\sigma_{\mathrm{ref}} = \eta\sigma_{\mathrm{nom}} \quad (6)$$

The reference multiplier, D, has unit of length, and can usually be defined by $D = \beta d$, where d is a conveniently chosen, "characteristic", component dimension. Therefore, for the known loading mode and component dimensions, σ_{nom} can be conveniently defined, and if the values of η and β are known, the corresponding equivalent uniaxial stress can be obtained by $\sigma_{\mathrm{ref}} = (\eta\sigma_{nom})$, and the corresponding uniaxial minimum creep strain rate can be obtained using eq. (5) if $\dot{\Delta}^c_{\mathrm{ss}}$ is known.

Determination of reference parameters

If an analytical solution can be obtained, substituting two values of n in the expression f_1 $(n)/\eta^n$ and equating the two resulting expressions allow the value of η to be determined. Hence, $\sigma_{\mathrm{ref}} = (\eta\sigma_{\mathrm{nom}})$ and D can be obtained. This approach was proposed by MacKenzie [18]. However, analytical solutions only exist for a small number of, usually, relatively simple components and loadings. If FE solutions to a creep problem are obtained ($\dot{\Delta}^c_{\mathrm{ss}}$) using several n values, but keeping all other material properties, loading and component dimensions the same, then σ_r can be obtained. This is done by taking several values of α, normalising the steady-state value of displacement rate, $\dot{\Delta}^c_{\mathrm{ss}}$, with respect to $A(\alpha\sigma_{\mathrm{nom}})^n$ and hence finding the value of α which renders $\left[\dot{\Delta}^c_{\mathrm{ss}}/(A(\alpha\sigma_{\mathrm{nom}})^n)\right]$ independent of n. This process is most easily visualised by plotting log $\left[\dot{\Delta}^c_{\mathrm{ss}}/(A(\alpha\sigma_{\mathrm{nom}})^n)\right]$ for various values of α against n, as illustrated in Figure 9. Also from Figure 9 it can be seen that, for very small n value, i.e. ($n \approx 0$), the straight lines produced using all of the α values have the same intercept on the log $\left[\dot{\Delta}^c_{\mathrm{ss}}/(A(\alpha\sigma_{\mathrm{nom}})^n)\right]$ axis. This intercept is equal to the logarithm of the reference multiplier, D.

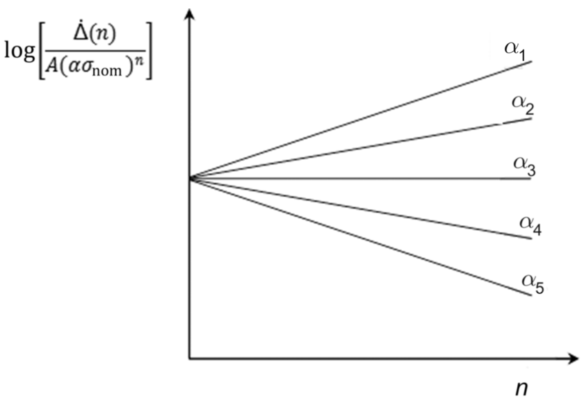

Figure 9: Variation of log steady-state creep displacement rate for various α values against n.

Equivalent gauge length

For a conventional uniaxial creep test, the creep strain at a given time is usually determined from the deformation of the GL. If the GL elongation is Δ and the elastic portion is neglected,

$$\varepsilon^{c} = \frac{\Delta}{\text{GL}} \tag{7a}$$

For non-conventional small specimen creep tests, an equivalent gauge length (EGL) [6–7] can be defined, if the measured creep deformation can be related to an equivalent uniaxial creep strain, in the same form as that of eq. (7a), i.e.

$$\varepsilon^{c} = \frac{\Delta}{\text{EGL}} \tag{7b}$$

The EGL is related to the dimensions of the specimen and in some cases may be related to the time-dependent deformation of the test specimen. The creep strain and creep deformation given in eq. (7b) may be presented in a form related to the reference stress, σ_{R}, i.e.

$$\varepsilon^{c}(\sigma_{\text{ref}}) = \frac{\Delta^{c}}{D} \tag{8}$$

in which $D\ (=\beta d)$ is the reference multiplier, which is, in fact, the EGL for the test. In some cases, the geometric changes, due to the specimen creep deformation with time, are small (e.g. for impression creep tests), and in such cases, the effects of geometric changes on D (EGL) can be neglected.

From eq. (8), an expression for the minimum creep strain rate can be obtained, i.e.

$$\dot{\varepsilon}^{c}(\sigma_{\text{ref}}) = \frac{\dot{\Delta}^{c}}{D} \tag{9}$$

in which $\dot{\varepsilon}^{c}$ is the minimum creep strain rate and $\dot{\Delta}^{c}$ is the minimum creep displacement rate.

Summary of the SNS4 and the OBS test procedure

The OBS testing method is based on the principle of converting the specimen load line displacement, displacement rate and displacement–time curves, to the corresponding uniaxial strain, strain rate and strain–time curves, using conversion relationships defined by eqs (6), (8) and (9). The conversion relationships, which are used to convert the specimen displacements and displacement rate to equivalent uniaxial strains and strain rate, are functions of specimen dimensions and deformations. The OBS and the SNS4 can be loaded using four loading pins, two of them are used to constrain the specimen and the other two are to apply tensile loading to the specimen as shown in Figures 5 and 7. The loading pins have to be attached to the loading machine using flexible joint, in order to allow good alignment to be achieved during the loading application. The loading fixtures generally have a much higher stiffness, compared to the specimen, and are generally manufactured from a material which has a much higher creep resistance than the tested material. The OBS and the SNS4 testing methods can be summarised as in the following points:

1. Small material samples are removed from the component surface or from the critical small regions, such as the HAZ or weld metal (WM) of weld, this small material sample is used to manufacture the SNS4 or the OBS.
2. Determine the conversion factors β and η, using FE analyses method for the particular OBS dimensions.
3. The OBS and the SNS4 are loaded using a tensile loading P, the load magnitude for the OBS is calculated for the required stress using η value for the specimen and specimen dimensions, i.e. eq. (6). For the SNS4 the applied load can be determined based on the required stress and the notched region dimensions.
4. The specimens are creep tested at the same practical operating temperature and stress levels much higher than the operating stress, this is to make the specimen fail in a shorter time.

5. The deformation of the SNS4 and the OBS is recorded throughout the test until the failure of the specimens.
6. The OBS deformation is converted to the corresponding uniaxial strain and strain rate using β value for the specimen and the conversion relationship, i.e. eqs (8) and (9).
7. These data then can be used to determine the creep strength for the components or the remaining lifetime, also it can be used to determine the creep constants for any creep model.

Finite element analysis

Material behaviour models

Norton's material model, i.e. $\dot{\varepsilon}^{c} = A\sigma^{n}$, was used in the FE analyses to obtain the minimum strain rate (MSR) for the OBS and the steady-state displacement rate ($\dot{\Delta}^{c}_{ss}$). This model was also used to determine the reference stress parameters β and η for the OBS. The Liu and Murakami model [19] is used to obtain full deformation–time creep curves for the OBS, the constitutive damage equations proposed by Liu–Murakami, i.e. eqs (10) and (11), introduce a damage parameter, ω, to represent the creep damage in the material. This model consists of a pair of coupled creep/damage equations, i.e.

$$\frac{d\varepsilon^{c}_{ij}}{dt} = \frac{3}{2}A\sigma_{eq}^{n-1}S_{ij}\exp\left[\frac{2(n+1)}{\pi\sqrt{1+3/n}}\left(\frac{\sigma_1}{\sigma_{eq}}\right)^{2}\omega^{3/2}\right] \tag{10}$$

$$\frac{d\omega}{dt} = \frac{M[1-\exp(-q_2)]}{q_2}(\sigma_r)^{\chi}\exp(q_2\omega) \tag{11}$$

The rupture stress σ_r, can be represented by eq. (12):

$$\sigma_r = \alpha'\sigma_1 + (1-\alpha')\sigma_{eq} \tag{12}$$

Integration of eq. (11), under uniaxial conditions, leads to

$$\omega = -\frac{1}{q_2}\ln\left[1-(1-e^{-q_2})\frac{t}{t_f}\right] \tag{13}$$

Also creep strain increments, for the uniaxial case, can be calculated using the following relationship:

$$\Delta\varepsilon^{c} = A\sigma^{n}\exp\left[\frac{2(n+1)}{\pi\sqrt{1+3/n}}\omega^{3/2}\right]\Delta t \tag{14}$$

where

$$t_f = \frac{1}{M\sigma^{\chi}} \tag{15}$$

where ω is the damage parameter ($0 < \omega < 1$), with $\omega = 0$ (no damage) and $\omega = 1$ (failure); the material constants A, n, M, χ and q_2 can be obtained by curve fitting to the uniaxial creep curves [14].

The material creep constants for P91 and P92 steels at 650°C, which are used in the FE analyses for the Liu and Murakami model, were reported in Ref. [14]. The FE analyses were carried out using the ABAQUS software package [20].

Specimen modelling

Three-dimensional FE analyses were carried out for the OBS using meshes which consist of 20-noded brick elements. Because of the symmetry, it was only necessary to model one quarter of the specimen and half of the specimen thickness, d, as shown in Figure 10. The boundary conditions, i.e. $u_x = 0$ on plane A, $u_y = 0$ on plane B and $u_z = 0$ on plane C, are also indicated in Figure 10. The specimen is loaded and constrained through four loading pins which are assumed to be "rigid" in the FE model. The applied load for the OBS was calculated for the required stress using eq. (6). FE analyses have been carried out to obtain full creep deformation–time curves using the OBS and the Liu and Murakami model.

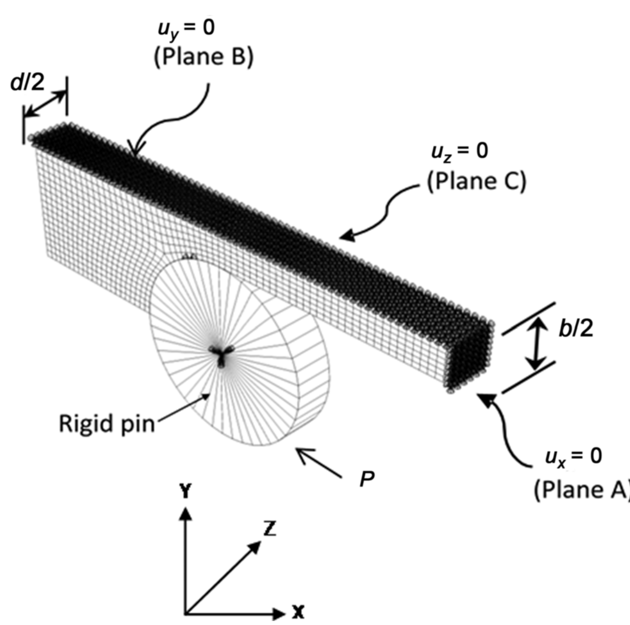

Figure 10: Finite element mesh and the boundary conditions for the OBS.

Determination of the reference stress parameters for the OBS

The FE analyses were used to determine the conversion factors η and β for the OBS. Accurate determination of the conversion factors allows the EGL and the corresponding uniaxial stress for the specimen to be accurately obtained. Using a Norton material model, i.e. $\dot{\varepsilon}^c = A\sigma^n$, FE analyses were performed to obtain the steady-state deformation rates between the loading pins for a range of n values, i.e. ($n = 8.2$, $n = 8.4$, $n = 8.6$, $n = 8.8$, $n = 9$, $n = 9.2$). Similar to Figure 11, the steady-state deformation rates between the loading pins, $\dot{\Delta}^c_{ss}$ are normalised by $L_o A\left(\eta \frac{P}{bd}\right)^n$, where P is the applied load. As only quarter of the specimen is used in the FE analyses and half of the specimen thickness, (see Figure 10), the obtained minimum deformation rates have to be doubled and the nominal stress will be $\frac{P}{0.25bd}$. Several η values were considered for all of the deformation rate values, with different n values, i.e. ($n = 8.2$, $n = 8.4$, $n = 8.6$, $n = 8.8$, $n = 9$, $n = 9.2$). The value of η which makes $\log\left(\frac{2\dot{\Delta}^c_{ss}}{L_o A\left(\eta \frac{P}{0.25bd}\right)^n}\right)$ practically independent of n is the required η value for the particular OBS geometry and dimensions. This value corresponds to the solid, horizontal line in Figure 11. The value of β can then be obtained from the intercept of the same solid line in Figure 11, with the vertical line, i.e. $\log\left(\frac{2\dot{\Delta}^c_{ss}}{L_o A\left(\eta \frac{P}{0.25bd}\right)^n}\right)$. This procedure is described in more detail in Ref. [14]. Using the same procedure the conversion factors, i.e. η and β, were fund to be 0.99 and 1.2, respectively, for the OBS with the dimensions of 13.0, 4.0, 2.0, 2.0, 7.0 and 5.0 mm, for L_o, k, b, d, H and D_i, respectively.

Validation

Initial validation of the OBS testing technique was carried out using 3D-FE analyses and Norton's law, to assess the accuracy of the conversion relationships, i.e. eqs (6), (8) and (9), and the conversion factors, i.e. η and β. The OBS steady-state deformation rates were obtained numerically using FE analyses for several n values, using Norton's model and FE analyses. The specimen steady-state deformation rates were converted to the MSR using eq. (9). The OBS dimensions, L_o, k, b, d, H and D_i, were 13.0, 4.0, 2.0, 2.0, 7.0 and 5.0 mm, respectively. These specimen dimensions result in conversion factors β and η values of 1.2 and 0.99, respectively. For this study the magnitude of the material constant A in Norton's law was 1.029E-20 for all cases, and the applied load corresponded to a constant stress of 50 MPa. The load was calculated using eq. (6) and the η value for the specimen which is 0.99. Using the same material properties, i.e. (A, n), and stress level, the MSRs have been obtained theoretically using Norton's model for several n values. The theoretical and numerical MSRs are plotted together in Figure 12;remarkably good correlation is found between the two sets of results.

To obtain a full deformation–time creep curve from the OBS, a continuum damage material behaviour model of Liu and Murakami has been used in the FE analysis, using the material constants for P91 and P92 steels at 650°C [19].Two high-temperature materials have been used in the validation, P91 and P92 steels, these materials are used extensively in the power plant pipework. For P91 five uniaxial creep tests have been performed at constant temperature of 650°C, under five stress levels, 70, 83, 87, 93 and 100 MPa. For P92 steel four uniaxial creep tests at constant temperature of 650°C have been performed, under four different stress levels 110, 120, 130 and

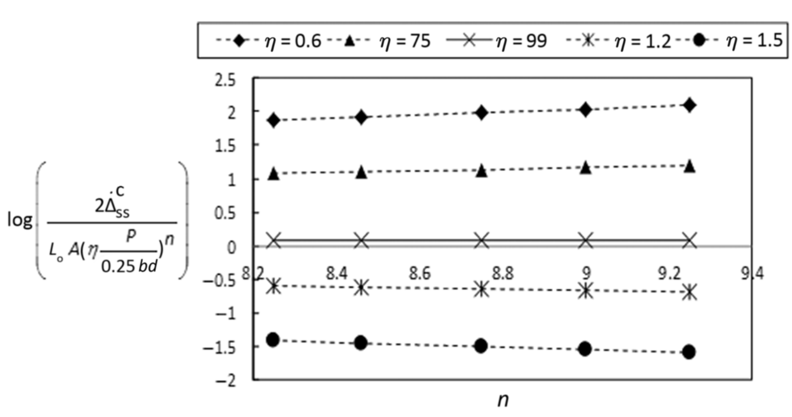

Figure 11: Determination of β and η parameters for the OBS.

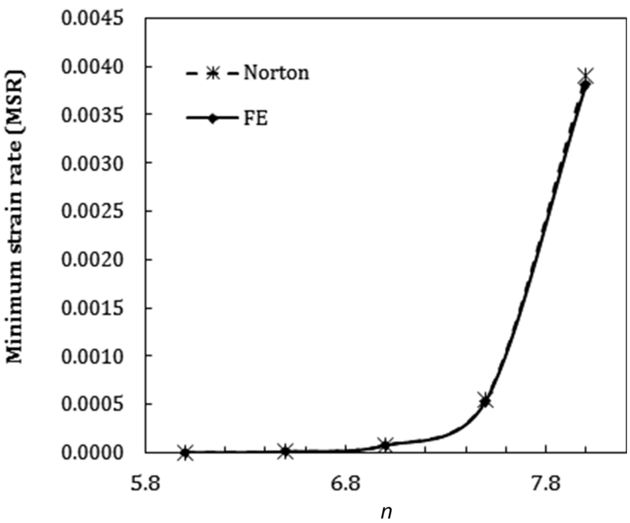

Figure 12: Comparison between the minimum strain rates (MSRs) obtained theoretically and numerically from the OBS.

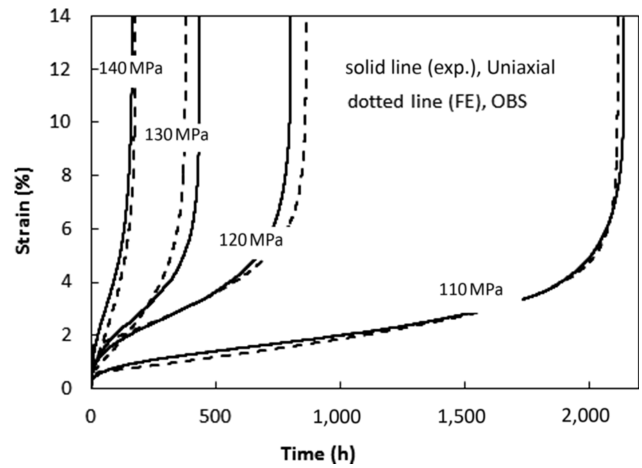

Figure 14: Creep strain–time curves obtained using (i) the FE converted results for the OBS and (ii) experimental uniaxial creep test results for P92 steel at 650°C.

140 MPa. The OBS creep deformation–time curves are converted to the strain–time curves using the relationship given by eq. (8) and the applied load is calculated using eq. (6). The conversion factors η and β for the tested OBS were 0.99 and 1.2, respectively. The tested OBS dimensions, L_o, k, b, d, H and D_i, were 13.0, 4.0, 2.0, 2.0, 7.0 and 5.0 mm, respectively. The converted OBS strain–time curves obtained from the FE analyses are compared with the corresponding uniaxial creep strain–time curves as in Figures 13 and 14;remarkably good correlation is found between the two results.

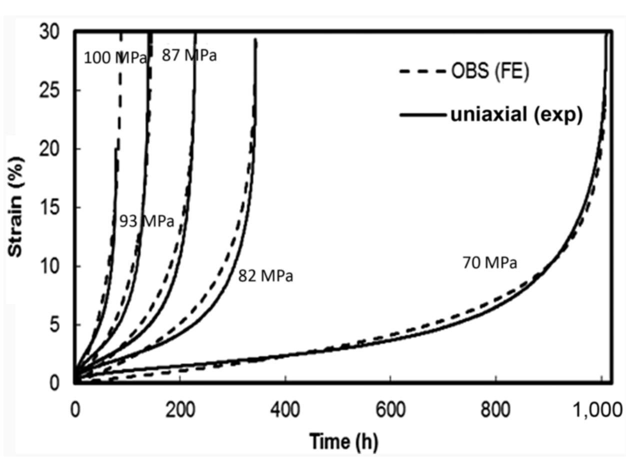

Figure 13: Creep strain–time curves obtained using (i) the FE converted results for the OBS and (ii) experimental uniaxial creep test results for P91 steel at 650°C.

Discussion

One of the main advantages of the OBS over other small specimen creep testing techniques is that, the specimen is capable of obtaining full creep strain–time creep curve using small material samples, such as the scoop samples removed from component surface from small material regions such as the HAZ of weld. The HAZ region is a very narrow region between the parent material (PM) and the WM, and there is no straight line boundary between the WM and HAZ also between the PM and the HAZ. Therefore, distinguishing the HAZ region from the WM and PM could be challenging. The OBS allows easy capturing of this region, because the OBS has very flexible design, the bar thickness (d) and depth (b) can be increased or decreased as required, in order to capture only the HAZ region, without increasing the risk of having significant deformation in the loading pin supporting material. This will allow accurate determination of the material creep properties. The OBS is unlike the TBS [14] where the loading pin supporting material behind the loading pins has to be large to avoid significant deformation; in the OBS the loading area, i.e. the contact area between the loading pins and the specimen, is relatively large in comparison to the bar cross-section area. This allows the OBS and the SNS4 to be machined from even smaller material samples; the specimens can be manufactured from the slides of materials removed, for example, from the HAZ region.

Conclusions

1. The OBS creep test is unlike other small specimen creep testing techniques, such as the small ring creep test and the impression creep test, where the test result is limited to the secondary creep region. The OBS creep test is capable of obtaining creep rupture data, the entire creep strain–time curve, i.e. primary, secondary and tertiary creep regions can be obtained.
2. The OBS FE results presented in Figures 12–14 indicate that the OBS is capable of obtaining full and accurate strain–time creep curves when compared with the uniaxial creep test results.
3. The OBS conversion relationships are material independent; therefore the high-temperature component creep strength can be assessed without any knowledge of its original creep properties.
4. The OBS and the SNS4 have simple geometry and they can be manufactured, loaded and tested easily.
5. The OBS and the SNS4 have the advantage of self-alignment during the loading application which increases the chance of obtaining accurate creep data.

Notation

$\varepsilon^c, \dot{\varepsilon}^c, \dot{\varepsilon}^c(\sigma_{ref})$	Creep strain, minimum creep strain rate and minimum creep strain rate at reference stress, respectively
$\Delta^c, \dot{\Delta}^c_{ss}$	Creep displacement and steady-state displacement rate
β, α, η	Reference parameters (conversion factors)
$\sigma, \sigma_r, \sigma_{ref}, \sigma_{nom}$	Stress, rupture stress, reference stress and nominal stress, respectively
A, n	Material constants in Norton's model
D	Reference multiplier
EGL	Equivalent gauge length
EDM	Electrical discharge machining
GL, d_{GL}	Gauge length and diameter of the gauge length, respectively
HAZ, WM, PM	Heat-affected zone, weld metal and parent material, respectively
FE	Finite element
SNS4	The small notched specimen with four loading pins
OBS	The pin-loaded small one-bar specimen
P, ω,α'	Applied load, damage parameter and multiaxial stress state parameter, respectively
A, n, M, χ and q_2	Material constants in Liu and Murakami model

References

[1] T.H. Hyde, A.A. Becker and W. Sun, Int. J. Pres. Ves. Pip., 83 (2006) 853–863.
[2] J.C.M. Li, Mater. Sci. Eng., A, 322 (2002) 23–42.
[3] R.G. Anderson, L.R.T. Gardener and W.R. Hodgkins, J. Mech. Eng. Sci., 5 (1963) 238–244.
[4] M. Saber, D.W.J. Tanner and W. Sun, J. Strain Anal. Eng., 46 (2011) 842–851.
[5] C.M. Davies, D.W. Dean, K.M. Nikbin and N.P.O. Dowd, Eng. Fract. Mech., 74 (2007) 882–897.
[6] S. Peravali, T.H. Hyde and K.A. Cliffe, J. Strain Anal., 43 (2008) 361–382.
[7] T.H. Hyde and W. Sun, J. Strain Anal., 44 (2009) 171–185.
[8] T.H. Hyde and W. Sun, Int J. Pres. Ves. Pip., 86 (2009) 757–763.
[9] M. Evans and D. Wang, J. Strain Anal., 42 (2007) 389–409.
[10] F. Hou, H. Xu, Y. Wang and L. Zhang, Eng. Fail. Anal., 28 (2013) 215–221.
[11] T.H. Hyde, B.S.M. Ali and W. Sun, J. Strain Anal. Eng. Des., 48 (2013) 269–278.
[12] B.J. Kim, Y.B. Sim, J.H. Lee, M.K. Kim and B.S. Lim, Procedia Eng., 10 (2011) 2579–2584.
[13] E. Fleury and J.S. Ha, Int. J. Pres. Ves. Pip., 75 (1998) 699–706.
[14] B.S.M. Ali, Development of Non-Destructive Small Specimen Creep Testing Techniques, Thesis submitted to The University of Nottingham, Nottingham, UK (2013), pp. 1–225.
[15] A. Garzillo, C. Guardamagna, L. Moscotti and L. Ranzani, Int. J. Pres. Ves. Pip., 66 (1996) 223–232.
[16] J.J. Williams and A.C.F. Cocks, J. Appl. Mech., 46 (1979) 795–799.
[17] A. Johnsson, Int. J. Mech. Sci., 16 (1974) 298–305.
[18] A.C. MacKenzie, Int. J. Mech. Sci., 10 (1968) 441–453.
[19] Y. Liu and S. Murakami, JSME Int. J. Ser. A, 41 (1998) 57–65.
[20] ABAQUS, ABAQUS 6.11-3 Standard User Manual, ABAQUS, Inc, USA, 2010.